## COMMUNICATION

# Graphite sulphate – a precursor to graphene†

Siegfried Eigler

**Graphite sulphate is used as a precursor to graphene for the first time. The positively charged graphene layers react with water to yield a processable graphene derivative. The unprecedented low density of defects is determined to be 0.06% on average and may open the way for electronic applications.**

Graphene is a nanomaterial of interdisciplinary interest and attracts attention of physicists as well as chemists or engineers.[1–3] Chemical vapour deposition is currently the method of choice to prepare large area graphene films and the quality is constantly increasing.[4] However, the wet-chemical synthesis of graphene is scalable and provides high potential for applications.[5,6]

Recently, the direct exfoliation of graphite in organic solvents attracted a lot of attention.[7,8] Although flakes of graphene ($G_1$) and few-layer graphene ($G_{few-layer}$) were wet-chemically produced by non-covalent exfoliation, the size of flakes is $<1$ μm and solvents with high boiling points are needed that limit the overall quality.[8] Graphene oxide (GO), an oxo-functionalised derivative of graphene, can be prepared on a large scale and mostly single layers with a reasonable size of flakes of several μm are obtained.[6] Furthermore, there is constant progress in improving functionalisation methods.[5,6,9] GO is also a potential precursor of graphene, however, with a variable amount of defects.[10,11] The quality of GO strongly depends on the synthetic protocol. Thus, GO can be amorphous, like humic acids, as a result of $CO_2$ formation due to over-oxidation, or the carbon framework remains almost intact by avoiding $CO_2$ formation during synthesis under certain reaction conditions.[6,10,12,13]

Generally, the quality of $G_1$ is limited by the density of defects within the carbon framework of GO.[11,14,15] Furthermore, defects in $G_1$ limit its performance in applications, such as electronic devices. Consequently, novel synthetic protocols have to be developed to further limit the formation of defects. The lowest density of defects

in GO, reported yet, is about 0.3% on average, as determined by statistical Raman microscopy (SRM).[6,11,16] The lowest density of defects of single flakes of GO is as low as 0.01%. Also the mobility of charge carriers depends on the density of defects of related $G_1$ and values of about 250 $cm^2$ $V^{-1}$ $s^{-1}$ are described for a density of defects of 0.3% and 1000 $cm^2$ $V^{-1}$ $s^{-1}$ for a density of defects of 0.01%.[6,10] However, to enter the field of electronic applications, such as sensor materials or transparent electrodes, the average quality of wet-chemically prepared $G_1$ must be enhanced. Also strong oxidants, such as potassium permanganate in sulfuric acid, commonly used to synthesise GO, bear some problems.[10,17,18] The reaction is exothermic and must be controlled by cooling and manganese salts are not environmentally friendly. Additionally, manganese impurities in graphene based materials should be avoided because they disturb their properties in applications.[19–21]

Here, it is demonstrated for the first time that processable oxo-functionalised graphene is yielded from graphite sulphate (Scheme 1), which is a precursor to $G_1$ and $G_{few-layer}$ with an unprecedented low density of defects of about 0.06% on average with a reasonable size of flakes of about 1–5 μm.

Recently, Dimiev *et al.* published the investigation of the formation of blue stage 1 graphite sulphate from natural graphite in sulphuric acid using persulphate as an oxidant (Scheme 1).[22,23] Although graphite sulphate is well known since decades,[24–27] it was not demonstrated to be a suitable precursor of oxo-functionalised graphene (oxo-$G_1$) or $G_1$ with a low density of defects. Rüdorff and Hofmann characterised graphite sulphate in depth,[25] and their analyses revealed an ideal structure of the stage 1 intercalation compound of $C_{24}^+HSO_4^- \cdot 2H_2SO_4$ (Scheme 1). It can be assumed that the positively charged $G_1$ layers in graphite sulphate can react with donors, such as water. However, up to now attempts failed to yield functionalised $G_1$, with lateral dimensions of several μm, confirmed by Raman spectroscopy.[28,29]

At first, graphite sulphate was prepared by the procedure described by Dimiev *et al.* from natural graphite in sulphuric acid by the addition of persulphate (Scheme 1).[22,23] The formation of graphite sulphate is confirmed by the colour change from black to blue (Fig. S1A, ESI†) and further confirmed by Raman spectroscopy.

*Department of Chemistry and Pharmacy and Institute of Advanced Materials and Processes (ZMP), Friedrich-Alexander-Universität Erlangen-Nürnberg (FAU), Dr.-Mack Str. 81, 90762 Fürth, Germany. E-mail: siegfried.eigler@fau.de; Fax: +49 (0)911 6507865015; Tel: +49 (0)911 6507865005*
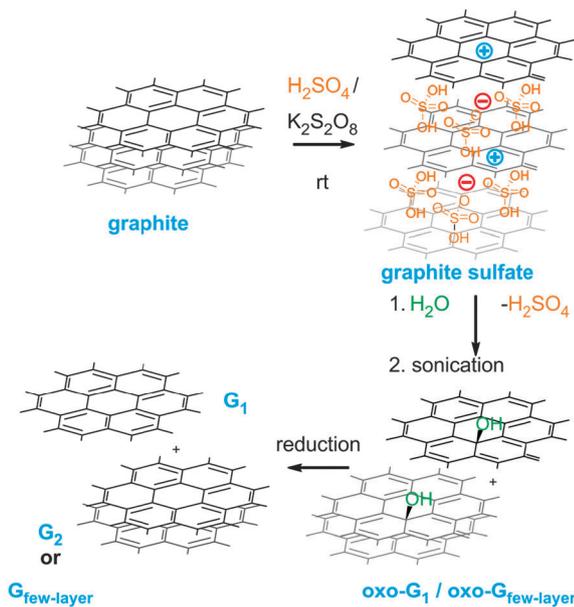
**Scheme 1** Synthesis of graphene ($G_1$) and few-layer graphene ($G_{few-layer}$) by the synthesis of graphite sulphate from natural graphite in sulfuric acid and persulphate under ambient conditions, followed by the reaction with water; sonication yields oxo-$G_1$ and oxo-$G_{few-layer}$; $G_1$ and $G_{few-layer}$ are yielded after reduction.



**Fig. 1** (A) Atomic force microscope (AFM) image of oxo-$G_1$ and oxo-$G_{few-layer}$; inset: height-profile along black and grey line. (B) UV/Vis spectrum of oxo-$G_1$ and oxo-$G_{few-layer}$. (C) Raman spectrum of a typical flake of oxo-$G_1$. (D) Thermogravimetric analysis of restacked oxo-functionalised graphene and temperature profiles of $m/z$ 18, 44 and 64.

A single Raman band at 1624 cm$^{-1}$ is observed as depicted in Fig. S1B (ESI†). After the formation of graphite sulphate, the reaction mixture was diluted with water, causing an increase in temperature to 60 °C. Excess of sulphuric acid and other salts were removed by repeated centrifugation and redispersion in water. The oxidation of graphite flakes was indicated by Raman spectroscopy by the defect induced broad D peak (Fig. S2, ESI†). Sonication of the oxidised particles in a mixture of water and methanol (1/1) caused exfoliation to oxo-$G_{few-layer}$ and even delamination to oxo-$G_1$. Larger particles were subsequently removed by centrifugation and the Langmuir–Blodgett technique was used to deposit flakes on a 300 nm SiO$_2$/Si wafer for analysis by atomic force microscopy (AFM) and SRM. In Fig. 1A the AFM image of oxo-$G_1$ and oxo-$G_{few-layer}$ is depicted (AFM overview shown in Fig. S3, ESI†). An area of 40.000 μm$^2$ of the film of flakes was investigated by SRM. The analysis of the disorder induced D peak, the G peak and the 2D peak confirms the absence of any graphene or unoxidised graphitic material as illustrated by the plot of $I_D/I_G$ against $\Gamma_D$ (Fig. S4, ESI†). Due to the functionalization in oxo-$G_1$ and oxo-$G_{few-layer}$ $\Gamma_D = 100 \pm 15$ cm$^{-1}$. The degree of functionalization is roughly estimated to be about 4%, as outlined below and in Table S1 (ESI†). UV/Vis spectra reveal an absorption band at 318 nm beneath 253 nm, which indicates residual unoxidised domains in oxo-$G_1$ and oxo-$G_{few-layer}$ (Fig. 1B). Furthermore, a C-content of 86% is determined by elemental analysis (EA) and also the mass-loss determined by thermogravimetric analysis (TGA) of 13% indicates the low degree of oxidation (Fig. 1D). An $m/z$ 64 is detected which relates to SO$_2$ formation at a decomposition temperature with a maximum at 380 °C, which originates most likely from organosulphate, as identified before.[30] The residual S-content determined by EA is 1.6% and thus, about 5% of the
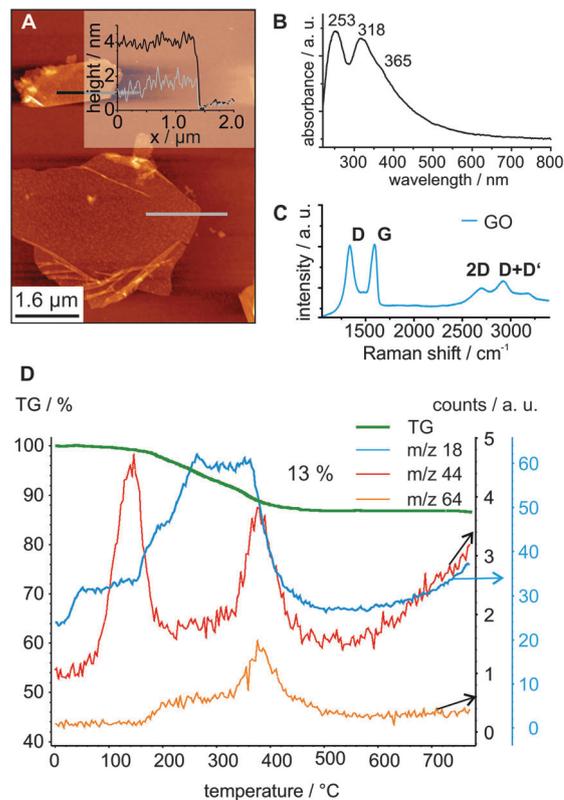
mass is related to organosulphate. This observation is in agreement with a recent study on the contamination of GO by chemical treatment.[19] TGA data further reveal that water is the major species detected between 250 °C and 350 °C which contributes mostly to the main weight-loss. A structure containing hydroxyl groups is further supported by FTIR spectroscopy (Fig. S5, ESI†). Consequently, a plausible structure of hydroxylated graphene with trapped water molecules and some organosulphate is proposed (Scheme 1).

Subsequently, the quality of $G_1$ was determined. Flakes of oxo-$G_1$ and oxo-$G_{few-layer}$ were deposited on a 300 nm SiO$_2$/Si wafer and exposed to vapour of hydroiodic acid and trifluoroacetic acid, a highly efficient reduction method suitable to generate $G_1$.[15] The flakes of $G_1$ and $G_{few-layer}$ were analyzed by AFM and the images reveal a height of $G_1$ of about 1 nm (Fig. 2B) and a typical size of flakes of approximately 1–5 μm (Fig. S6, ESI†). The $G_1$ nature of flakes was confirmed by Raman spectroscopy and the density of defects within the carbon framework of $G_1$ was also evaluated. Raman spectra of $G_1$ exhibit a G and 2D peak in addition to a defect induced D peak. The full-width at half-maximum ($\Gamma$) of the 2D peak is a criterion to identify single layers of $G_1$ by a value < 40 cm$^{-1}$.[31–33] Furthermore, spectra of $G_{few-layer}$ can be filtered by the intensity of the G peak.[16] For the first time, the SRM analysis of data probed from an area of 250.000 μm$^2$ reveals that 79% of Raman spectra of $G_1$ (out of 2873 spectra) show a
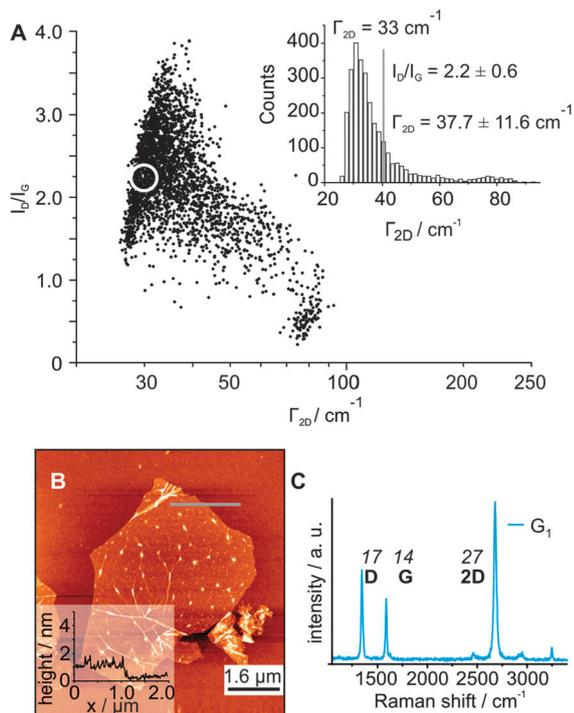
**Fig. 2** (A) SRM analysis of a film of flakes of $G_1$ (plot of $I_D/I_G$ against $\Gamma_{2D}$, spectra of $G_{few\text{-}layer}$ filtered by $I_G$) which indicates the high quality of $G_1$ by the narrow average $\Gamma_{2D}$ values of $< 40$ cm$^{-1}$; inset: histogram of $\Gamma_{2D}$ with the maximum of $\Gamma_{2D} = 33$ cm$^{-1}$. (B) AFM image of $G_1$ derived from oxo-$G_1$; inset: height-profile along the grey line. (C) Raman spectrum of $G_1$, $\Gamma_{D,G,2D}$ in italic numbers.

$\Gamma_{2D} < 40$ cm$^{-1}$ (Fig. 2A). The $\Gamma_{2D}$ values of analyzed spectra indicate a maximum in the histogram at 33 cm$^{-1}$ depicted in the inset of Fig. 2A. A typical Raman spectrum of $G_1$ is presented in Fig. 2C with a $\Gamma_{2D} = 27$ cm$^{-1}$. The relation of Raman data and the density of defects was introduced by Lucchese and Cançado and allows estimating the density of defects to about 0.06% on average.[31,34] In comparison, the best average quality of $G_1$ prepared from GO with an almost intact carbon framework (ai-GO) was 0.3%.[10] The here presented data indicate the best average quality, with a density of defects of 0.06% with a μm size of flakes ($^{1-5\mu m, 0.06\%}G_1$). The reaction of graphite sulphate with water was also conducted at $< 10$ °C, conditions used for the pre-paration of ai-GO.[10] SRM data reveal a slightly increased quality of $G_1$ with a density of defects of about 0.04% (Fig. S7, ESI†). Unfortunately, the yield of $G_1$ prepared here can only be estimated, because of contamination with $G_{few\text{-}layer}$. However, SRM data reveal that about 25% of flakes are $G_1$ and improve-ment of separation techniques will increase the part of $G_1$. Furthermore, the amount of $G_1$ isolated from 1 g of graphite is on the mg scale but may be suitable for the development of sensor materials.

It can be concluded that the positively charged carbon layers of graphite sulphate can be functionalised under ambient reaction conditions with water as a donor. The multi-layered material readily delaminates in water–methanol to oxo-$G_1$ and oxo-$G_{few\text{-}layer}$. The degree of functionalization is roughly esti-mated to be approximately 4% and hydroxyl groups beneath

some organosulphate groups are proposed. Although the yield of dispersed $G_1$ and $G_{few\text{-}layer}$ is improvable, the size of flakes is 1–5 μm, suitable even for applications, such as sensor devices. For the first time, an unprecedented low average density of defects of 0.06% was determined for wet-chemically prepared flakes of $G_1$ and all Raman spectra of $G_1$ exhibit a sharp 2D peak. Although the potential of this type of oxo-$G_1$ is not yet explored, it can be assumed that it is a precursor to $G_1$ suitable for functionalization. Also the reactivity of $G_1$ and the influence of defects can be evaluated and the field of electronic applications is within reach.

## Notes and references

1 W. Ren and H. M. Cheng, *Nat. Nanotechnol.*, 2014, **9**, 726–730.
2 A. H. Castro Neto, N. M. R. Peres, K. S. Novoselov and A. K. Geim, *Rev. Mod. Phys.*, 2009, **81**, 109–162.
3 K. S. Novoselov, V. I. Fal'ko, L. Colombo, P. R. Gellert, M. G. Schwab and K. Kim, *Nature*, 2012, **490**, 192–200.
4 Y. Hao, M. S. Bharathi, L. Wang, Y. Liu, H. Chen, S. Nie, X. Wang, H. Chou, C. Tan, B. Fallahazad, H. Ramanarayan, C. W. Magnuson, E. Tutuc, B. I. Yakobson, K. F. McCarty, Y. W. Zhang, P. Kim, J. Hone, L. Colombo and R. S. Ruoff, *Science*, 2013, **342**, 720–723.
5 D. R. Dreyer, A. D. Todd and C. W. Bielawski, *Chem. Soc. Rev.*, 2014, **43**, 5288–5301.
6 S. Eigler and A. Hirsch, *Angew. Chem., Int. Ed.*, 2014, **53**, 7720–7738 (*Angew. Chem.*, 2014, **126**, 7852–7872).
7 Y. Hernandez, V. Nicolosi, M. Lotya, F. Blighe, Z. Sun, S. De, I. T. McGovern, B. Holland, M. Byrne, Y. Gun'Ko, J. Boland, P. Niraj, G. Duesberg, S. Krishnamurti, R. Goodhue, J. Hutchison, V. Scardaci, A. C. Ferrari and J. N. Coleman, *Nat. Nanotechnol.*, 2008, **3**, 563–568.
8 K. R. Paton, E. Varrla, C. Backes, R. J. Smith, U. Khan, A. O'Neill, C. Boland, M. Lotya, O. M. Istrate, P. King, T. Higgins, S. Barwich, P. May, P. Puczkarski, I. Ahmed, M. Moebius, H. Pettersson, E. Long, J. Coelho, S. E. O'Brien, E. K. McGuire, B. M. Sanchez, G. S. Duesberg, N. McEvoy, T. J. Pennycook, C. Downing, A. Crossley, V. Nicolosi and J. N. Coleman, *Nat. Mater.*, 2014, **13**, 624–630.
9 M. Segal, *Nat. Nanotechnol.*, 2009, **4**, 612–614.
10 S. Eigler, M. Enzelberger-Heim, S. Grimm, P. Hofmann, W. Kroener, A. Geworski, C. Dotzer, M. Rockert, J. Xiao, C. Papp, O. Lytken, H. P. Steinrück, P. Müller and A. Hirsch, *Adv. Mater.*, 2013, **25**, 3583–3587.
11 S. Eigler, S. Grimm, M. Enzelberger-Heim, P. Müller and A. Hirsch, *Chem. Commun.*, 2013, **49**, 7391–7393.
12 A. Dimiev, D. V. Kosynkin, L. B. Alemany, P. Chaguine and J. M. Tour, *J. Am. Chem. Soc.*, 2012, **134**, 2815–2822.
13 A. M. Dimiev and J. M. Tour, *ACS Nano*, 2014, **8**, 3060–3068.
14 S. Eigler, S. Grimm and A. Hirsch, *Chem. – Eur. J.*, 2014, **20**, 984–989.
15 S. Eigler, *Phys. Chem. Chem. Phys.*, 2014, **16**, 19832–19835.
16 S. Eigler, F. Hof, M. Enzelberger-Heim, S. Grimm, P. Müller and A. Hirsch, *J. Phys. Chem. C*, 2014, **118**, 7698–7704.
17 G. Charpy, *C. R. Hebd. Séances Acad. Sci.*, 1909, **148**, 920–923.
18 J. William, S. Hummers and R. E. Offeman, *J. Am. Chem. Soc.*, 1958, **80**, 1339.
19 C. K. Chua, A. Ambrosi, Z. Sofer, A. Mackova, V. Havranek, I. Tomandl and M. Pumera, *Chem. – Eur. J.*, 2014, **20**, 15760–15767.
20 C. H. Wong, Z. Sofer, M. Kubesova, J. Kucera, S. Matejkova and M. Pumera, *Proc. Natl. Acad. Sci. U. S. A.*, 2014, **111**, 13774–13779.
21 L. Wang, A. Ambrosi and M. Pumera, *Angew. Chem., Int. Ed.*, 2013, **52**, 13818–13821 (*Angew. Chem.*, 2013, **125**, 14063–14066).
22 A. M. Dimiev, G. Ceriotti, N. Behabtu, D. Zakhidov, M. Pasquali, R. Saito and J. M. Tour, *ACS Nano*, 2013, **7**, 2773–2780.

23 A. M. Dimiev, S. M. Bachilo, R. Saito and J. M. Tour, *ACS Nano*, 2012, **6**, 7842–7849.
24 C. Schafhaeutl, *J. Prakt. Chem.*, 1840, **21**, 129–157.
25 W. Rüdorff and U. Hofmann, *Z. Anorg. Allg. Chem.*, 1938, **238**, 1–50.
26 M. S. Dresselhaus and G. Dresselhaus, *Adv. Phys.*, 2002, **51**, 1–186.
27 T. Enoki, M. Suzuki and M. Endo, *Graphite Intercalation Compounds and Applications*, Oxford University Press, Oxford, 2003.
28 N. I. Kovtyukhova, Y. Wang, A. Berkdemir, R. Cruz-Silva, M. Terrones, V. H. Crespi and T. E. Mallouk, *Nat. Chem.*, 2014, **6**, 957–963.
29 J. Zheng, C. A. Di, Y. Liu, H. Liu, Y. Guo, C. Du, T. Wu, G. Yu and D. Zhu, *Chem. Commun.*, 2010, **46**, 5728–5730.
30 S. Eigler, C. Dotzer, F. Hof, W. Bauer and A. Hirsch, *Chem. – Eur. J.*, 2013, **19**, 9490–9496.
31 L. G. Cançado, A. Jorio, E. H. M. Ferreira, F. Stavale, C. A. Achete, R. B. Capaz, M. V. O. Moutinho, A. Lombardo, T. S. Kulmala and A. C. Ferrari, *Nano Lett.*, 2011, **11**, 3190–3196.
32 S. Chen, W. Cai, R. D. Piner, J. W. Suk, Y. Wu, Y. Ren, J. Kang and R. S. Ruoff, *Nano Lett.*, 2011, **11**, 3519–3525.
33 S. Lee, K. Lee and Z. Zhong, *Nano Lett.*, 2010, **10**, 4702–4707.
34 M. M. Lucchese, F. Stavale, E. H. M. Ferreira, C. Vilani, M. V. O. Moutinho, R. B. Capaz, C. A. Achete and A. Jorio, *Carbon*, 2010, **48**, 1592–1597.